Quantum transport in a one-dimensional quantum dot array

W. Z. Shangguan, T. C. Au Yeung, Y. B. Yu, and C. H. Kam
School of Electrical and Electronic Engineering, Nanyang Technological University, Singapore, 639798
(Received 4 October 2000; revised manuscript received 7 November 2000; published 31 May 2001)

In this paper we study electronic transport through a quantum dot array containing an arbitrary number of quantum dots connected in a series by tunnel coupling under dc bias. The on-site Coulomb interaction is ignored. The retarded self-energy of any dot in the array is made up of left and right components and is of staircase type, terminating at corresponding electron reservoirs. We calculate the dc current based on the nonequilibrium Green's function formalism developed by Jauho *et al.* [A.-P. Jauho, Ned S. Wingreen, and Y. Meir, Phys. Rev. B **50**, 5528 (1994)]. The dc current in both finite and infinite number dots in the array is calculated. The electronic spectrum of the system is found to fall within an interval centered at ϵ_0 (the dot energy level) with a width of two times the tunnel coupling amplitude between two neighboring dots. The electronic charge in each dot is plotted for the finite number dot array.

DOI: 10.1103/PhysRevB.63.235323 PACS number(s): 73.61.−r, 05.60.Gg, 66.35.+a, 72.20.Ht

I. INTRODUCTION

Quantum dots are man-made ''droplets'' of charge that contain anything from a single electron to a collection of several thousand.[1] The electronic states in dots can be probed by transport when a tunnel coupling is allowed between the dot and a nearby source and drain leads. The physics of quantum dots shows many parallels with the behavior of naturally occurring quantum systems in atomic, nuclear, and condensed-matter physics. Indeed, quantum dots exemplify an important trend in condensed-matter physics in which researchers study man-made objects rather than real atoms or nuclei. As electronic confinement in quantum dots approaches atomic dimensions, behaviors characteristic of atomic impurities have emerged, such as the quantization of the electronic spectrum and the electronic charge, which plays a major role in the physics of nanostructures. With quantum dots, experimentalist can perform experiments that were difficult to realize even inaccessible by simply changing a voltage. One such example is the quantum dot as a magnetic impurity in condensed-matter physics.[1]

In the last decade much work has been contributed to the system of a single quantum dot connected to two electron reservoirs. Many authors have studied the transport properties[1–10] and capacitance spectroscopy[11] in order to probe the discrete electronic spectrum of the system. Among the transport properties one notable feature is the Kondo effect.[1–4] Meir *et al.* have shown that the on-site Coulomb interaction leads to the Kondo effect and hence the Kondo peak in differential conductance[4] and to the Coulomb-blockade conductance oscillations.[5,6] By measuring the Coulomb oscillations of current, Tarucha *et al.*[7] have studied the shell filling and spin effect in a quantum dot, showing that the addition sequence of electrons to the dot is similar to Hund's rule.

In recent years, research interest has extended to systems of multiple dots.[12–22] For example, electron pumping was studied in a double dot with interdot capacitance;[12] the Kondo effect in a double dot with on-site Coulomb interaction was studied based on the slave-boson mean-field theory;[18] and the dc current of a double dot without on-site Coulomb interaction was derived by Kawamura and Aono.[15] Recently, Ivanov[14] has studied dc transport through nonequilibrium double quantum dots at low-temperature and shown how the Kondo peaks in the spectral density evolve with the interdot tunneling amplitude T_M; Pohjola *et al.*[13] have investigated the resonant tunneling through double quantum dots in the presence of strong Coulomb repulsion and coupling to the metallic leads. Using a real-time diagrammatic formulation they evaluated the spectral density and the nonlinear conductance and showed a novel triple-peak resonant structure in the conductance.

In this paper we study a system of one-dimensional quantum dot arrays containing an arbitrary number of quantum dots connected in a series by tunnel coupling. Our formalism is based on the nonequilibrium Green's function proposed by Jauho *et al.*[25] As the dot number in the array becomes very large, even infinite, the system we are considering resembles in many ways a one-dimensional lattice. This system is of much interest as a new artificial material. When the electron density is held low in an array of very small quantum dots, electron-phonon scattering is expected to be suppressed by gaps between subbands,[23] in contrast to an array of quantum dots in which many electrons are confined by the depletion regions of a semiconductor.[24] This is because a quantum dot confined by a heterostructure can be made so small as the order of 10 nm. Chen *et al.* studied the metal to antiferromagnetic insulator transition of a two-dimensional quantum dot lattice.[21] Much earlier, Ugajin investigated the nature of the electric-field-induced Mott metal-insulator transition in a quantum dot array.[22] To the best of our knowledge, however, there has so far not been a systematic calculation on the density of states and the differential conductance of a quantum dot array system. It is the purpose of this paper to calculate the ''lesser'' and retarded Green's functions for the one-dimensional quantum dot array containing $N+2$ dots connected by tunnel coupling, where N can be any positive integer, and to derive an analytical formula for the current under the dc bias voltage.

In Sec. II we calculate the dc response of the system, including the case of infinite N. We calculate in Sec. III the electronic charge of an arbitrary dot in the dot array for a finite N. Numerical results and analysis are presented in Sec. IV, and the main conclusions are addressed in Sec. V.

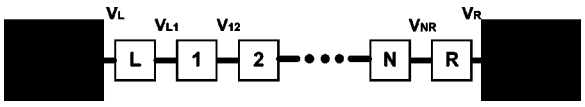

FIG. 1. A quantum dot array of $N+2$ dots connected in a series by an interdot tunnel coupling is connected to two electron reservoirs.

II. dc RESPONSE

Let us consider a system of one-dimensional quantum dot array connected to two electron reservoirs. The array consists of $N+2$ quantum dots connected in a series by tunnel coupling, as shown in Fig. 1. For notational convenience we call the first and the last dot in the array the left L and the right R dot, respectively. The Hamiltonian H of the system is given by

$$H=\sum_{k,\alpha\in L,R}\epsilon_{k\alpha}c_{k\alpha}^{\dagger}c_{k\alpha}+\sum_{i=L,R,1}^{N}\epsilon_i^0 d_i^{\dagger}d_i+\sum_{i=1}^{N}V_{i,i+1}(d_i^{\dagger}d_{i+1}+\text{H.c.})+V_L(c_{kL}^{\dagger}d_L+\text{H.c.})+V_R(c_{kR}^{\dagger}d_R+\text{H.c.}), \tag{1}$$

where $c_{k\alpha}^{\dagger}$ ($c_{k\alpha}$) is the creation (annihilation) operator for electrons in α reservoir, $d_i^{\dagger}$ (d_i) is the electron creation (annihilation) operator within the ith quantum dot, V_L (V_R) is the tunneling coupling between the left (right) dot and the left (right) reservoir, and $V_{i,i+1}$ is the tunneling coupling between the ith and $(i+1)$th dots. The electron spin index is suppressed.

The ''lesser'' and retarded Green's functions are defined by

$$G_{i,i}^{<}(t)=i\langle d_i^{\dagger}(0)d_i(t)\rangle, \tag{2}$$

$$G_{i,i}^{r}(t)=-i\theta(t)\langle\{d_i(t),d_i^{\dagger}(0)\}\rangle \quad (i=L,1,2,\ldots,N,R). \tag{3}$$

A. General formalism

By the method of equations of motion and Keldysh's contour integration, we obtain the following equations for the retarded Green's function:

$$G_{LL}^{r}=g_{LL}^{r}+g_{LL}^{r}\Sigma_L^{r}G_{LL}^{r}+g_{LL}^{r}\Sigma_{L1}G_{1L}^{r}, \tag{4}$$

$$G_{RR}^{r}=g_{RR}^{r}+g_{RR}^{r}\Sigma_R^{r}G_{RR}^{r}+g_{RR}^{r}\Sigma_{RN}G_{NR}^{r}, \tag{5}$$

$$G_{i\alpha}^{r}=g_{ii}^{r}\Sigma_{i,i-1}G_{i-1,\alpha}^{r}+g_{ii}^{r}\Sigma_{i,i+1}G_{i+1,\alpha}^{r}, \tag{6}$$

$$G_{Li}^{r}=g_{LL}^{r}\Sigma_L^{r}G_{Li}^{r}+g_{LL}^{r}\Sigma_{L1}G_{1i}^{r} \tag{7}$$

$$G_{Ri}^{r}=g_{RR}^{r}\Sigma_R^{r}G_{Ri}^{r}+g_{RR}^{r}\Sigma_{RN}G_{Ni}^{r}, \tag{8}$$

$$G_{RL}^{r}=g_{RR}^{r}\Sigma_R^{r}G_{RL}^{r}+g_{RR}^{r}\Sigma_{RN}G_{NL}^{r}. \tag{9}$$

In the above $\alpha=i,L,R$ and $i=1,2,\ldots,N$, $\Sigma_{\alpha\beta}$'s are self-energies arising from electron tunneling between the nearest-neighboring αth and βth quantum dots; the free-particle Green's functions in each dot are defined by

$$g_{i,i}^{<}(t,t')=i\langle d_i^{\dagger}(t')d_i(t)\rangle, \tag{10}$$

$$g_{i,i}^{r}(t,t')=-i\theta(t-t')\langle\{d_i(t),d_i^{\dagger}(t')\}\rangle \quad (i=L,1,2,\ldots,N,R) \tag{11}$$

and the self-energies for the left and right dot are defined by

$$\Sigma_L^{r,a,<}(t,t')=V_L^2\sum_k g_{kL}^{r,a,<}(t,t'), \tag{12}$$

$$\Sigma_R^{r,a,<}(t,t')=V_R^2\sum_k g_{kR}^{r,a,<}(t,t'), \tag{13}$$

which are associated with the tunneling between the left reservoir and the left dot and that between the right reservoir and the right dot, respectively. The Green's functions $g_{kL}^{r,a,<}(t,t')$ and $g_{kR}^{r,a,<}(t,t')$ in Eqs. (12) and (13) correspond to free electrons in the left and right reservoir, respectively.

Equation (9) can be rewritten as

$$G_{RL}^{r}=G_{RR}^{r0}V_{RN}G_{NL}^{r}, \tag{14}$$

where $G_{\alpha\alpha}^{r0}$ is defined by

$$G_{\alpha\alpha}^{r0}(\omega)\equiv\frac{1}{\omega-\epsilon_\alpha^0-\Sigma_\alpha^r(\omega)} \quad (\alpha=L,R). \tag{15}$$

Using Eqs. (6) and (14) by back substitution from G_{NL}^{r} to G_{LL}^{r} one arrives at

$$G_{LL}^{r}(\omega)=\cfrac{1}{\omega-\epsilon_L^0-\Sigma_L^r(\omega)-\cfrac{V_{L1}^2}{\omega-\epsilon_1^0-\cfrac{V_{12}^2}{\omega-\epsilon_2^0-\cfrac{V_{23}^2}{\ddots\;\cfrac{V_{N-1,N}^2}{\omega-\epsilon_N^0-\cfrac{V_{NR}^2}{\omega-\epsilon_R^0-\Sigma_R^r(\omega)}}}}}}. \tag{16}$$

The result presented in Eq. (16) has an obvious physical interpretation. The retarded Green's function for the left quantum dot, which connects directly to the left electron reservoir and dot 1 to its right by tunnel coupling, is of the form $G^r_{LL}(\omega)=1/[(g^r_{LL})^{-1}-\vec{\Sigma}^r_{LL}-\vec{\Sigma}^r_{LL}]$, where g^r_{LL} is the unperturbed Green's function of the left dot, while the retarded self-energy of the left quantum dot is composed of two parts: the ''left self-energy'' $\vec{\Sigma}^r_{LL}(\omega)$ which is simply $\Sigma^r_L(\omega)$ expressed in Eq. (12) and can be rewritten as

$$\vec{\Sigma}^r_{LL}(\omega)=\sum_k \frac{V_L^2}{(g^r_{kL})^{-1}},$$

and the ''right self-energy'' which is of the form $\vec{\Sigma}^r_{LL}=1/[(g^r_{11})^{-1}-\vec{\Sigma}^R_{11}]$, where $(g^r_{11})^{-1}$ and $\vec{\Sigma}^R_{11}$ are the unperturbed Green's function and the ''right retarded self-energy'' of dot 1, respectively. As dot 1 is connected to dot 2 to its right the ''right retarded self-energy'' of dot 1 is modified by $\vec{\Sigma}^R_{11}=1/[(g^r_{22})^{-1}-\vec{\Sigma}^R_{22}]$ (here $\vec{\Sigma}^R_{22}$ is the right retarded self-energy of dot 2) instead of $1/[(g^r_{22})^{-1}]$, . . . , ending up with the right electron reservoir at $\Sigma^r_R(\omega)=\Sigma_k V^2_L/[(g^r_{kL})^{-1}]$. For the ''left self-energy'' of any quantum dot, it terminates at the left electron reservoir. When the quantum dot array reduces to only one dot connected to the left and right lead, a case that has been theoretically and experimentally investigated intensively, the retarded self-energy for the dot is simply $\Sigma^r=\Sigma_k\{V^2_L/(g^r_{kL})^{-1}+V^2_R/(g^r_{kR})^{-1}\}$, thus our result is consistent with that obtained previously, see, for example, Ref. 25. For the case of $N=0$, i.e., the two-dot case, our result is identical to that of Kawamura *et al.*[15] Hence, the retarded Green's function for any dot site in the quantum dot array under dc bias can be easily worked out. If we define

$$G^{r0}_{ii}\equiv \cfrac{1}{\omega-\epsilon^0_i-\cfrac{V^2_{i,i+1}}{\omega-\epsilon^0_{i+1}-\cfrac{V^2_{i+1,i+2}}{\omega-\epsilon^0_{i+2}-\cfrac{V^2_{i+2,i+3}}{\ddots\ \cfrac{V^2_{N-1,N}}{\omega-\epsilon^0_N-\cfrac{V^2_{NR}}{\omega-\epsilon^0_R-\Sigma^r_R(\omega)}}}}}} \quad (i=1,2,\ldots,N), \tag{17}$$

then the following relation can be obtained:

$$\begin{aligned} G^r_{LL}(\omega)-G^a_{LL}(\omega) &= -i\Gamma^L(\omega)|G^r_{LL}|^2-i\Gamma^R(\omega)V^2_{L1}V^2_{12}V^2_{23}\cdots V^2_{N-1,N}V^2_{NR} \\ &\quad\times|G^r_{LL}|^2|G^{r0}_{11}|^2|G^{r0}_{22}|^2\cdots|G^{r0}_{NN}|^2|G^{r0}_{RR}|^2 \end{aligned} \tag{18}$$

in which the identity

$$\Sigma^r_\alpha(\omega)-\Sigma^a_\alpha(\omega)=-i\Gamma^\alpha(\omega) \quad (\alpha=L,R) \tag{19}$$

and Eq. (17) have been employed. From Eqs. (6) and (14), using the same iteration technique, we have

$$\begin{aligned} G^r_{RL}(\omega) &= V_{L1}V_{12}\cdots V_{N-1,N}V_{NR}G^r_{LL}(\omega) \\ &\quad\times G^{r0}_{11}(\omega)\cdots G^{r0}_{NN}(\omega)G^{r0}_{RR}(\omega). \end{aligned} \tag{20}$$

In the above derivations we have used interchangeably $\Sigma_{ij}(=V_{ij})=\Sigma_{ji}(=V_{ji})$ for $i,\ j=L,1,2,\ldots N,R$.

Next, we shall calculate the ''lesser'' Green's function. Similarly by contour integration we have

$$G^<_{LL}(\omega)=G^{r0}_{LL}\Sigma^<_L G^a_{LL}+G^{r0}_{LL}\Sigma_{L1}G^<_{1L}, \tag{21}$$

$$G^<_{iL}=g^r_{ii}\Sigma_{i-1,i}G^<_{i-1,L}+g^r_{ii}\Sigma_{i,i+1}G^<_{i+1,L}, \tag{22}$$

$$G^<_{RL}(\omega)=G^{r0}_{RR}\Sigma^<_R G^a_{RL}+G^{r0}_{RR}\Sigma_{RN}G^<_{NL}, \tag{23}$$

where G^{r0}_{LL} and G^{r0}_{RR} have been defined by Eq. (15) while the lesser self-energy $\Sigma^<_\alpha(\omega)=if_\alpha(\omega/\hbar)\Gamma^\alpha(\omega)$ $(\alpha=L,R)$. Here $f_\alpha(\omega/\hbar)$ is the Fermi function of the electron reservoirs given by $f_\alpha(\omega/\hbar)=1/(e^{\beta(\hbar\omega-\mu_\alpha)}+1)$, where $\beta=1/kT$ and μ_α is chemical potential. Again by back substitution from $G^<_{NL}$ to $G^<_{LL}$, we get

$$\begin{aligned} G^<_{LL}(\omega) &= |G^r_{LL}|^2\Sigma^<_L+V^2_{L1}V^2_{12}\cdots V^2_{NR} \\ &\quad\times|G^r_{LL}|^2|G^{r0}_{11}|^2\cdots|G^{r0}_{NN}|^2|G^{r0}_{RR}|^2\Sigma^<_R. \end{aligned} \tag{24}$$

In the above derivation, the expression for $G^r_{RL}(\omega)$ in Eq. (20) has been used. Combining Eqs. (18) and (24) the ''lesser'' Green's function for the left quantum dot can be expressed as

$$\begin{aligned} G^<_{LL}(\omega) &= i(f_L(\omega)-f_R(\omega))\Gamma^L(\omega)|G^r_{LL}(\omega)|^2 \\ &\quad -f_R(\omega)(G^r_{LL}(\omega)-G^a_{LL}(\omega)). \end{aligned} \tag{25}$$

The left current J_L flowing from the left electron reservoir into the dot array can be expressed compactly by[20]

$$J_L=\frac{2e}{h}\int d\epsilon(f_L(\epsilon)-f_R(\epsilon))T(\epsilon), \tag{26}$$

where the transmission probability $T(\epsilon)$ is given by

$$\begin{aligned}T(\epsilon)=&\Gamma^L\left(\frac{\epsilon}{\hbar}\right)\Gamma^R\left(\frac{\epsilon}{\hbar}\right)V_{L1}^2V_{12}^2\cdots V_{NR}^2\\&\times\left|G_{LL}^r\left(\frac{\epsilon}{\hbar}\right)\right|^2\left|G_{11}^{r0}\left(\frac{\epsilon}{\hbar}\right)\right|^2\left|G_{22}^{r0}\left(\frac{\epsilon}{\hbar}\right)\right|^2\cdots\\&\left|G_{NN}^{r0}\left(\frac{\epsilon}{\hbar}\right)\right|^2\left|G_{RR}^{r0}\left(\frac{\epsilon}{\hbar}\right)\right|^2.\end{aligned} \tag{27}$$

In the above equation $\Gamma^L(\epsilon/\hbar)=2\pi V_L^2\rho_L(\epsilon)$ [$\rho_L(\epsilon)$ is the density of states of electrons in the left reservoir] is the coupling of the left dot to the left electron reservoir. We have a similar definition for $\Gamma^R(\epsilon/\hbar)$ for the right electron reservoir. With Eqs. (25) and (24) and by some simple derivations we obtain

$$\begin{aligned}J_L=&-\frac{e}{\hbar}\int\frac{d\epsilon}{2\pi}[f_L(\epsilon)-f_R(\epsilon)]\Gamma^L\left(\frac{\epsilon}{\hbar}\right)\\&\times\left\{2\,\mathrm{Im}[G_{LL}^r(\epsilon)]+\Gamma^L\left(\frac{\epsilon}{\hbar}\right)|G_{LL}^r(\epsilon)|^2\right\}.\end{aligned} \tag{28}$$

Equations (28) and (16) establish close formulas for the calculation of the dc current. As expected, the expression for the nonequilibrium dc response of the quantum dot array is a Landauer-like formula, with the transmission probability proportional to the coupling between the quantum dot array and the electron reservoirs, as one can see from Eq. (27).

B. Infinite quantum dot array

We consider in this section the case of infinite quantum dots in the array. We assume $V_{L1}=V_{12}=\cdots=V_{N-1,N}=V_{NR}=V$ and $\epsilon_i^0=\epsilon_0$ for $i=1,2,\ldots,N$. From Eq. (16) the retarded Green's function for the left quantum dot can then be rewritten as

$$G_{LL}^r=\frac{1}{\omega-\epsilon_L^0-\Sigma_L^r(\omega)-\vec{\Sigma}_{LL}^r}, \tag{29}$$

where $\vec{\Sigma}_{LL}^r=V^2G_{11}^{r0}$ and G_{11}^{r0} is defined by Eq. (17).[26] As the quantum dot array contains infinite dots, the ''right self-energy'' $\vec{\Sigma}_{LL}^r$ can be written as

$$\vec{\Sigma}_{LL}^r=\frac{V^2}{\omega-\epsilon_0-\vec{\Sigma}_{LL}^r} \tag{30}$$

which yields the solution

$$\vec{\Sigma}_{LL}^r=\frac{(\omega-\epsilon_0)\pm\Delta}{2}, \tag{31}$$

where Δ is defined by

$$\Delta=\sqrt{(\omega-\epsilon_0)^2-4V^2}. \tag{32}$$

The solution for $\vec{\Sigma}_{LL}^r$ in Eq. (31) has two branches. As $\vec{\Sigma}_{LL}^r$ and $\vec{\Sigma}_{LL}^a$ fulfill the same equation (30), we can write simply as $\vec{\Sigma}_{LL}=(\omega-\epsilon_0+\Delta)/2$; when Δ is in the upper complex plane, the solution corresponds to $\vec{\Sigma}_{LL}^r$ while in lower complex plane $\vec{\Sigma}_{LL}^a$. Substituting Eq. (31) into Eq. (29) directly one obtains

$$G_{LL}^r=\frac{2}{2[\omega-\epsilon_L^0-\Sigma_L^r(\omega)]-(\omega-\epsilon_0)-\Delta}. \tag{33}$$

By writing Eq. (33) we have assumed that Δ is in the upper complex plane.

Alternatively, one may also solve G_{LL}^r by relating $\vec{\Sigma}_{LL}^r$ to G_{LL}^r and then substituting into Eq. (29). Two methods give identical results for $\vec{\Sigma}_{LL}^r$ and G_{LL}^r.

The dc current of the quantum dot array with infinite quantum dots again can be calculated by Eq. (28), while the retarded Green's function G_{LL}^r in this case is given by Eq. (33).

It is worthwhile to point out that in the infinite dot case and without couplings of the quantum dot array with electron reservoirs, i.e., $\Sigma_L^r(\omega)=\Sigma_R^r(\omega)=0$, our system becomes identical to the one-dimensional lattice system. In this case the retarded Green's function in each dot can be shown to be the same as that for the one-dimensional lattice system, which was given in the book by Economou.[27]

III. ELECTRONIC CHARGE IN EVERY DOT

In the preceding section we have worked out the retarded Green's functions for every quantum dot in the one-dimensional $N+2$ dots array. We now proceed to calculate the electronic charge in an arbitrary dot in the array, which entails a lesser Green's function for every dot in the dot array. We begin with the retarded Green's function of each dot in the array. For the ith dot in the array, its retarded Green's function is given by

$$G_{ii}^r=\frac{1}{\omega-\epsilon_i^0-V_{i,i-1}^2\tilde{G}_{i-1,i-1}^{r0}-V_{i,i+1}^2\tilde{G}_{i+1,i+1}^{r0}}, \tag{34}$$

where $\tilde{G}_{i,i}^{r0}$ and $\vec{G}_{i,i}^{r0}$, respectively, are defined by

$$\begin{aligned}\vec{G}_{i,i}^{r0}=&\cfrac{1}{\omega-\epsilon_i^0-\cfrac{V_{i,i+1}^2}{\omega-\epsilon_{i+1}^0-\cfrac{V_{i+1,i+2}^2}{\ddots\cfrac{V_{N-1,N}^2}{\omega-\epsilon_N^0-\cfrac{V_{NR}^2}{\omega-\epsilon_R^0-\Sigma_R^r(\omega)}}}}},\end{aligned} \tag{35}$$

$$\tilde{G}^{r0}_{i,i}=\cfrac{1}{\omega-\epsilon^0_i-\cfrac{V^2_{i,i-1}}{\omega-\epsilon^0_{i-1}-\cfrac{V^2_{i-1,i-2}}{\ddots\;\cfrac{V^2_{21}}{\omega-\epsilon^0_L-\cfrac{V^2_{L1}}{\omega-\epsilon^0_L-\Sigma^r_L(\omega)}}}}}, \tag{36}$$

As it is a little lengthy to calculate the lesser Green's function of the arbitrary ith quantum dot, in the following we give only the final result, the detailed derivation is presented in the Appendix. We have

$$\begin{aligned} G^<_{ii}(\omega)=&V^2_{L1}V^2_{12}\cdots V^2_{i-1,i}\\ &\times|\tilde{G}^{r0}_{LL}|^2|\tilde{G}^{r0}_{11}|^2|\tilde{G}^{r0}_{22}|^2\cdots|\tilde{G}^{r0}_{i-1,i-1}|^2|G^r_{ii}|^2\Sigma^<_L\\ &+V^2_{i,i+1}V^2_{i+1,i+2}\cdots V^2_{N-1,N}V^2_{NR}\\ &\times|G^r_{ii}|^2|\vec{G}^{r0}_{i+1,i+1}|^2\cdots|\vec{G}^{r0}_{N-1,N-1}|^2\\ &\times|\vec{G}^{r0}_{NN}|^2|\vec{G}^{r0}_{RR}|^2\Sigma^<_R. \end{aligned} \tag{37}$$

For expression symmetry we have rewritten G^{r0}_{LL} and G^{r0}_{RR}, which are defined in Eq. (15), as $\tilde{G}^{r0}_{LL}$ and $\vec{G}^{r0}_{RR}$, respectively. When $i=L$, the above result reduces to Eq. (24) for the left quantum dot. Noting that $V^2_{i,i-1}\tilde{G}^{r0}_{i-1,i-1}$ and $V^2_{i,i+1}\vec{G}^{r0}_{i+1,i+1}$ is, respectively, the ''left'' and ''right'' retarded self-energy of dot i, if we write

$$G^<_{ii}(\omega)=G^r_{ii}(\omega)\Sigma^<_{ii}(\omega)G^a_{ii}(\omega)$$

then the lesser self-energy $\Sigma^<_{ii}(\omega)$ of dot i can be then written by

$$\begin{aligned} \Sigma^<_{ii}=&\Sigma^<_L|\tilde{\pi}^r_{11}|^2|\tilde{\pi}^r_{22}|^2\cdots|\tilde{\pi}^r_{ii}|^2\\ &+|\vec{\pi}^r_{ii}|^2\cdots|\vec{\pi}^r_{N-1,N-1}|^2|\vec{\pi}^r_{NN}|^2\Sigma^<_R, \end{aligned} \tag{38}$$

where $\tilde{\pi}^r_{ii}=V_{i,i-1}\tilde{G}^{r0}_{i-1,i-1}$ and $\vec{\pi}^r_{ii}=V_{i,i+1}\vec{G}^{r0}_{i+1,i+1}$ are equal to the left and right retarded self-energy of the ith dot divided by $V_{i,i-1}$ and $V_{i,i+1}$, respectively.

The electronic charge in the ith quantum dot in the $N+2$ quantum dot array can be calculated by

$$Q_i=\int\frac{d\omega}{2\pi}\mathrm{Im}[G^<_{ii}(\omega)]. \tag{39}$$

Equations (39) and (34)–(37) form a close set of formulas to calculate the electronic charge in an arbitrary dot site in the $N+2$ dot array.

IV. NUMERICAL RESULTS

In this section we present some numerical results of differential conductance as well as the electronic charge in every dot in the quantum dot array. In the wide-band limit, the linewidth function $\Gamma^\alpha(\omega)$ ($\alpha\in L,R$) are energy-independent constants, and we assume $\Gamma^L(\omega)=\Gamma^R(\omega)=\Gamma$ in our numerical calculations, and the level shift now is zero. We assume also $V_{L1}=V_{12}=\cdots=V_{N-1,N}=V_{NR}=V$ and $\epsilon^0_i=\epsilon_0$ for $i=L,1,2,\ldots,N,R$. The differential conductance is calculated numerically by setting the right Fermi level μ_R fixed ($\mu_R=0$).[4,5]

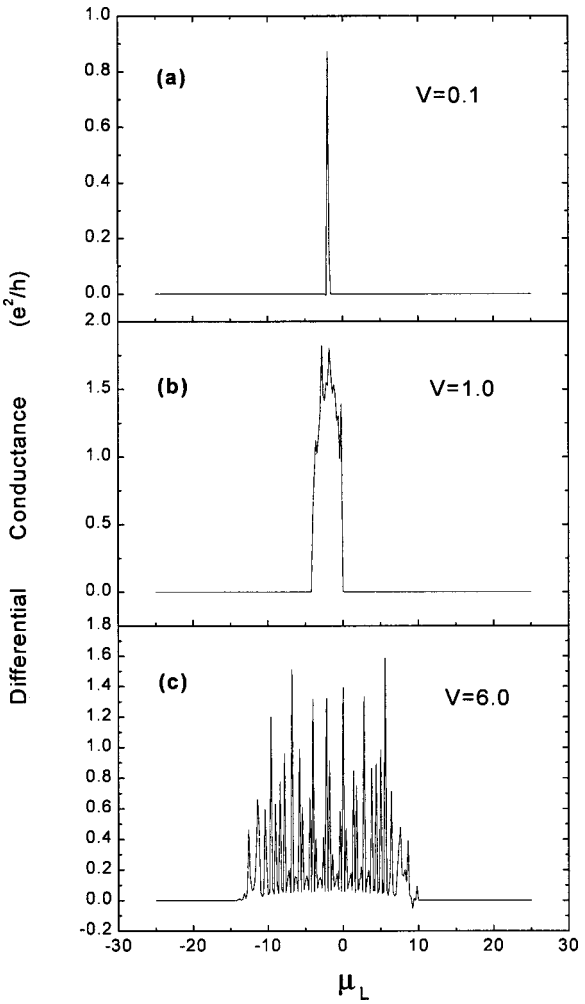

FIG. 2. Plot of the differential conductance against the left Fermi level for $N=100$, with $\beta=100$, $\epsilon_0=-2.0$ at different inter-dot tunnel couplings: (a) $V=0.1$, (b) $V=1.0$, (c) $V=6.0$. All energies are expressed by units of Γ.

In Figs. 2 and 3 we plot the differential conductance with respect to the chemical potential of the left reservoir with dot number $N=100$ in the array for three different tunnel coupling amplitudes of $V=0.1$, 1.0, and 6.0. The energy level of dots ϵ_0 is set to -2.0 (all energies are measured with respect to μ_R). At low temperature [Fig. 2(a)–2(c)], when V is small, the differential conductance shows only a sharp peak pinned at ϵ_0 [Fig. 2(a)]. When V is large, the conductance peak splits into multiple ones; the maximum number of the peaks is equal to the total dot number when V is sufficiently large for a given finite N. In all cases the peaks of differential conductance are within the interval of $\epsilon_0\pm 2V$. When the temperature is high (Fig. 3), however, the differential conductance peaks become round and show a single round peak

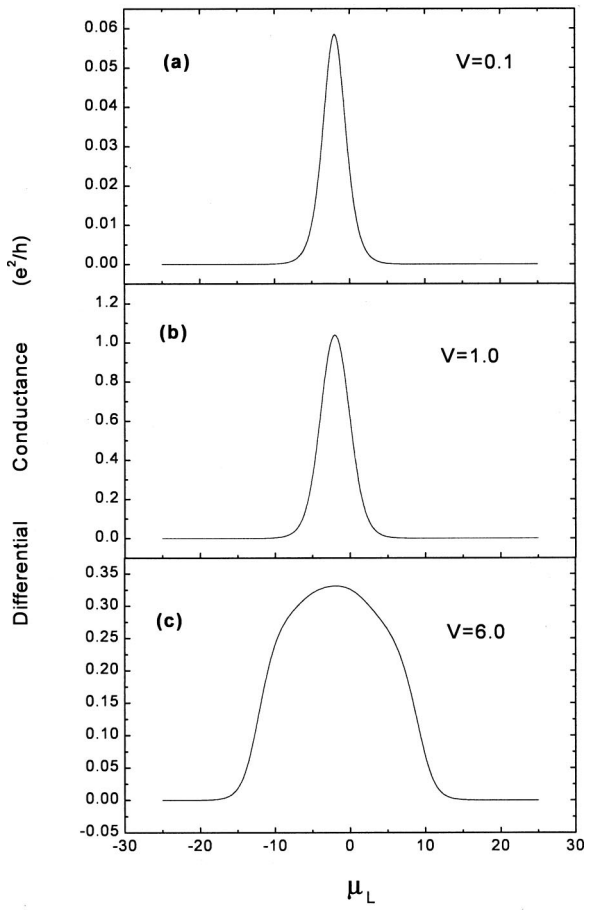

FIG. 3. Plot of the differential conductance against the left Fermi level for $N=100$, with $\beta=1$, $\epsilon_0=-2.0$ at different interdot tunnel couplings: (a) $V=0.1$, (b) $V=1.0$, (c) $V=6.0$. All energies are expressed by units of Γ.

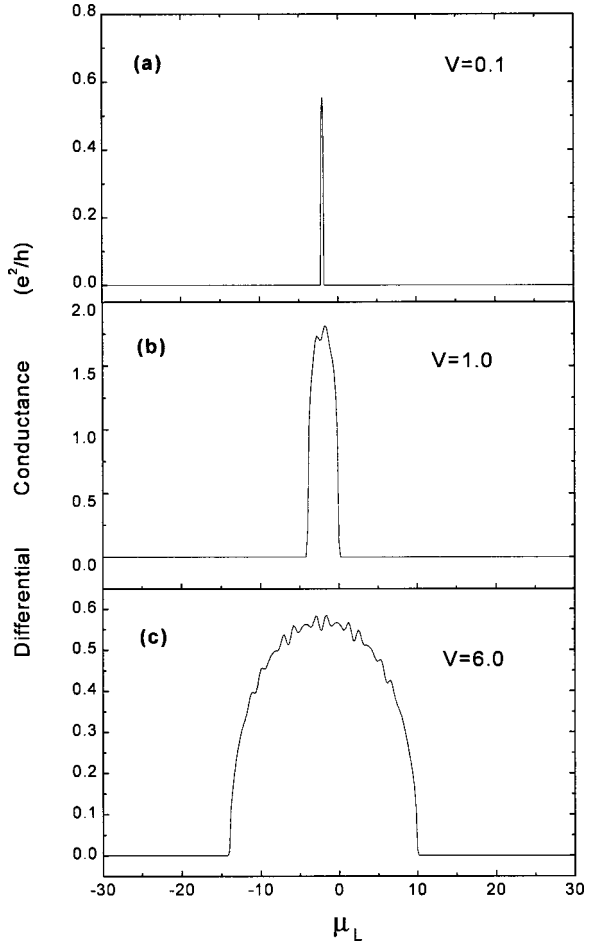

FIG. 4. Plot of the differential conductance against the left Fermi level for an infinite dot array, with $\beta=100$, $\epsilon_0=-2.0$ at different interdot tunnel couplings: (a) $V=0.1$, (b) $V=1.0$, (c) $V=6.0$. All energies are expressed by units of Γ.

pinned again at ϵ_0, but the peaks width are broadened and slightly exceed the range of $\epsilon_0 \pm 2V$, while in all three cases the heights of the peaks reduce considerably. As expected, at low temperature, the system is basically within the Coulomb blockade regime. As the Fermi level of the left reservoir rises to a higher level that equals some energy level of the quantum dot array, the differential conductance has a peak, but this is restricted by the tunnel coupling strength between dots, which determines the electronic spectrum of the system. For intermediate tunnel coupling ($V=1.0$), the differential conductance peak reaches almost 2, which means perfect transparency of the quantum dot lattice. At high temperature, however, the energy levels of the system that are otherwise at low temperature becomes blurred and even continuous; this leads to a round conductance peak which reaches its maximum when the Fermi level of the left reservoir equals to ϵ_0. We expect this because small V means most electrons supplied by the left reservoir to the dot L turn back before they go forward to the other dots. Thus the electrons see only a single quantum dot in this case. The energy level that they belong to is simply $\epsilon_0=-2.0$. Clearly, the single peak in the density of states is due to the coupling of the dot array to the electron reservoirs. For large V the electrons oscillate frequently among all the dots in the array before they tunnel into the reservoirs. The energy levels of the electrons should be identical to those of an isolated $N+2$ dot. That is, there should be $N+2$ peaks in the density of states. The couplings Γ^L and Γ^R broaden the $N+2$ peaks.

Next we consider the infinite quantum dot case. At low temperature (Fig. 4), the differential conductance vanishes outside the range of $\epsilon_0 \pm 2V$, while at high temperature (Fig. 5), the peaks of the differential conductance are again broadened and fall quickly outside the interval of $\epsilon_0 \pm 2V$, as shown in Fig. 5. Unlike the case of a finite quantum dot, the differential conductance plot does not oscillate violently with μ_L; only when V is large is there some small fluctuations in the top.

In Fig. 6 we plot the electronic charge in every dot in the quantum dot array. The parameters are $\epsilon_0=-2.0$, $\mu_L=-2.5$, $N=49$. Three tunnel coupling amplitudes are considered. For small V, most of the electrons that enter the right dot will bounce back into the right reservoir. So there is lots of charge accumulates in the dots and there is a tiny current flowing through all the dots. As a result, the charge distribution over all the dots is almost 1.0, while in the dots near the left reservoir, the charge begins to decrease. From the figure one can see the charge decreases significantly from about 0.8

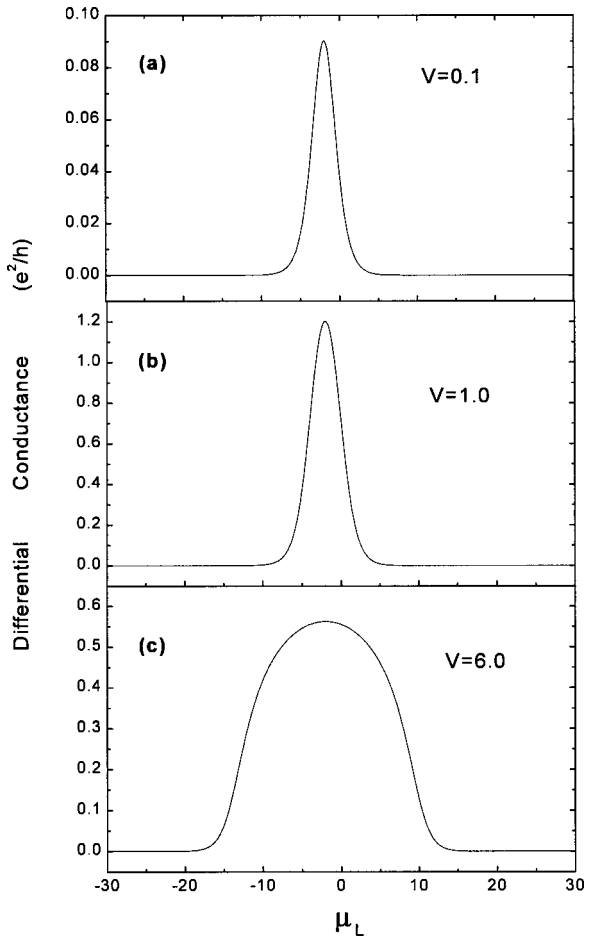

FIG. 5. Plot of the differential conductance against the left Fermi level for an infinite dot array, with $\beta=1$, $\epsilon_0=-2.0$ at different interdot tunnel couplings: (a) $V=0.1$, (b) $V=1.0$, (c) $V=6.0$. All energies are expressed by units of Γ.

in dot 1 to 0.3 in the left dot. This is because the left dot connects directly to the left reservoir, and the tunnel coupling between the left dot and the left reservoir in this case is much larger than that between the intermediate dots. The same applies to the sharp decline in the right dot for small V.

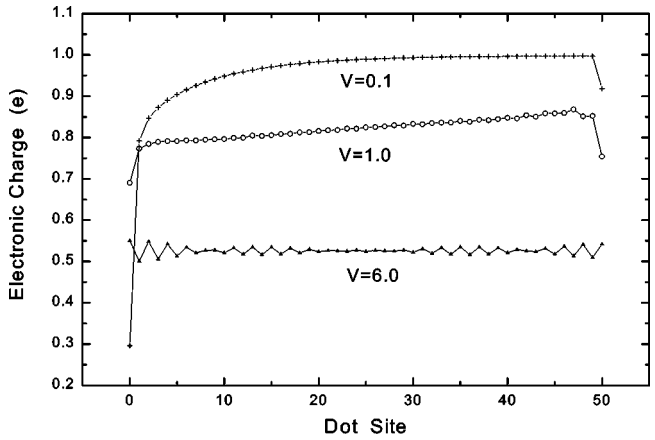

FIG. 6. Plot of the electronic charge for a 51-dot quantum dot array with different interdot tunnel couplings $V=0.1$, 1.0, and 6.0. The remaining parameters are the same as in Fig. 5.

For the intermediate V, most of the electrons from the reservoir can only enter the last few dots and then they will bounce back into the right reservoir. There is a small current passing through all the dots. Apart from the last three dots, the electronic charge distribution declines steadily from dot 47 to dot 1. As the case of $V=0.1$, there is also a sharp decrease of charges between dot 1 and the left dot, but in this case, the decrease amplitude is much less than that of $V=0.1$.

When V is very large, however, most of the electrons that enter the right dot from the right reservoir can pass easily through all the dots. Hence, there is a large current through the system, as one can tell from Fig. 2(c). This leads to an almost flat charge distribution over all dots; but there are small fluctuations between dots, this may be caused by the variation of the electric field among different dots as the tunnel coupling is strong.

V. CONCLUSIONS

We have studied nonequilibrium quantum transport through a one-dimensional quantum dot lattice under dc bias voltage. Both finite and infinite number dot cases are studied. The electronic spectrum of the system is found to be within the interval of two times the tunnel coupling amplitude at low temperature. The electronic charge in the first and last dot differs prominently from that in the dot in between when the interdot tunnel coupling is small, and the charge distribution fluctuates among dots when it is large.

The technique we have developed in this paper is simple but powerful. Although we demonstrate here only a one-dimensional quantum dot lattice, the technique should be capable of tackling two- and three-dimensional quantum dot lattices to study their transport properties, electronic spectrum, and other properties as well.

ACKNOWLEDGMENTS

W.Z.S. is grateful to Dr. Chu Yun Chung and Lee Wing Foon for numerical computation aid.

APPENDIX A: ''LESSER'' GREEN'S FUNCTION FOR AN ARBITRARY DOT

Similar to the calculation for $G^<_{LL}$, one begins with the following equations:

$$G^<_{Li}=G^{r0}_{LL}\Sigma^<_L G^a_{Li}+G^{r0}_{LL}\Sigma_{L1}G^<_{1i}, \tag{A1}$$

$$G^<_{ni}=g^r_{nn}\Sigma_{n,n-1}G^<_{n-1,i}+g^r_{nn}\Sigma_{n,n+1}G^<_{n+1,i}$$

$$(n=1,2,\ldots,N), \tag{A2}$$

$$G^<_{Ri}=G^{r0}_{RR}\Sigma^<_R G^a_{Ri}+G^{r0}_{RR}\Sigma_{RN}G^<_{Ni}. \tag{A3}$$

By forward substitution, we first substitute $G^<_{Li}$ into the equation for $G^<_{1i}$, relating $G^<_{1i}$ to $G^<_{2i}$, . . . , until $G^<_{i-1,i}$ which is expressed as

$$G^<_{i-1,i}=\tilde{G}^{r0}_{i-1,i-1}V_{i-1,i}G^<_{ii}+V_{i-1,i-2}\cdots V_{21}V_{1L}\times\tilde{G}^{r0}_{i-1,i-1}\cdots\tilde{G}^{r0}_{22}\tilde{G}^{r0}_{11}G^{r0}_{LL}\Sigma^<_L G^a_{Li}. \quad (A4)$$

In the above equation $\tilde{G}^{r0}_{ii}$ is defined by Eq. (36). And similarly by back substitution from $G^<_{Ri}$ to $G^<_{ii}$ we have

$$G^<_{i,i}=\vec{G}^{r0}_{ii}V_{i,i-1}G^<_{i-1,i}+V_{i,i+1}V_{i+1,i+2}\cdots V_{N-1,N}V_{NR}\times\vec{G}^{r0}_{i+1,i+1}\cdots\vec{G}^{r0}_{N-1,N-1}\vec{G}^{r0}_{NN}G^{r0}_{RR}\Sigma^<_R G^a_{Ri}, \quad (A5)$$

where $\vec{G}^{r0}_{ii}$ is defined by Eq. (35). Equations (A4) and (A5) imply that

$$G^<_{i,i}=\frac{1}{1-V^2_{i,i-1}\tilde{G}^{r0}_{i-1,i-1}\vec{G}^{r0}_{ii}}\times(V_{L1}V_{12}\cdots V_{i-1,i}\tilde{G}^{r0}_{LL}\tilde{G}^{r0}_{11}\cdots\tilde{G}^{r0}_{i-1,i-1}\vec{G}^{r0}_{ii}\Sigma^<_L G^a_{Li}+V_{i,i+1}V_{i+1,i+2}\cdots V_{NR}\times\vec{G}^{r0}_{ii}\vec{G}^{r0}_{i+1,i+1}\cdots\vec{G}^{r0}_{NN}\vec{G}^{r0}_{RR}\Sigma^<_R G^a_{Ri}). \quad (A6)$$

Now we have to calculate G^a_{Li} and G^a_{Ri} which are involved in the above equation. We begin with the following equations:

$$G^r_{Li}=G^{r0}_{LL}\Sigma_{L1}G^r_{1i}, \quad (A7)$$

$$G^r_{ni}=g^r_{nn}\Sigma_{n,n-1}G^r_{n-1,i}+g^r_{nn}\Sigma_{n,n+1}G^r_{n+1,i}\quad(n=1,2,\ldots,N), \quad (A8)$$

$$G^r_{Ri}=G^{r0}_{RR}\Sigma_{RN}G^r_{Ni}. \quad (A9)$$

From Eqs. (A7)–(A9) we obtain

$$G^r_{Li}=V_{L1}V_{12}\cdots V_{i-1,i}G^{r0}_{LL}\tilde{G}^{r0}_{11}\tilde{G}^{r0}_{22}\cdots\tilde{G}^{r0}_{i-1,i-1}G^r_{ii}, \quad (A10)$$

$$G^r_{Ri}=V_{RN}V_{N,N-1}\cdots V_{i+1,i}G^{r0}_{RR}\vec{G}^{r0}_{NN}\cdots\vec{G}^{r0}_{i+1,i+1}G^r_{ii}. \quad (A11)$$

Substituting the complex conjugate of Eqs. (A10) and (A11) into Eq. (A6) and noting that

$$\frac{\vec{G}^{r0}_{ii}}{1-V^2_{i,i-1}\tilde{G}^{r0}_{i-1,i-1}\vec{G}^{r0}_{ii}}=G^r_{ii}, \quad (A12)$$

the ''lesser'' Green's function for the arbitrary dot site in the quantum dot array is then obtained,

$$G^<_{ii}(\omega)=V^2_{L1}V^2_{12}\cdots V^2_{i-1,i}\times|\tilde{G}^{r0}_{LL}|^2|\tilde{G}^{r0}_{11}|^2\cdots|\tilde{G}^{r0}_{i-1,i-1}|^2|G^r_{ii}|^2\Sigma^<_L+V^2_{i,i+1}V^2_{i+1,i+2}\cdots V^2_{NR}|G^r_{ii}|^2\times|\vec{G}^{r0}_{i+1,i+1}|^2\cdots|\vec{G}^{r0}_{NN}|^2|\vec{G}^{r0}_{RR}|^2\Sigma^<_R. \quad (A13)$$

[1] D. Goldhaber-Gorden, Hadas Shtrikman, D. Mahalu, David Abusch-Magder, U. Meirav, and M.A. Kastner, Nature (London) **391**, 156 (1998); S. M. Cronenwett, T.H. Oosterkamp, and L.P. Kouwenhoven, Science **281**, 540 (1998).

[2] Y.B. Yu, T.C. Au Yeung, W.Z. Shangguan, and C.H. Kam, Phys. Lett. A **275**, 131 (2000).

[3] D.C. Ralph and R.A. Buhrman, Phys. Rev. Lett. **72**, 3401 (1994); T.K. Ng, *ibid.* **76**, 487 (1996).

[4] Y. Meir, N.S. Wingreen, and P.A. Lee, Phys. Rev. Lett. **70**, 2601 (1993); N.S. Wingreen and Y. Meir, Phys. Rev. B **49**, 11 040 (1994).

[5] Y. Meir, Ned S. Wingreen, and P.A. Lee, Phys. Rev. Lett. **66**, 3048 (1991).

[6] C.W.J. Beenakker, Phys. Rev. B **44**, 1646 (1991).

[7] S. Tarucha, D.G. Austing, T. Honda, R.J. van der Hage, and L.P. Kouwenhoven, Phys. Rev. Lett. **77**, 3613 (1996).

[8] A.T. Johnson, L.P. Kouwenhoven, W.de Jong, N.C. van der Vaart, C.J.P.M. Harmans, and C.T. Foxon, Phys. Rev. Lett. **69**, 1592 (1992).

[9] P.L. McEuen, E.B. Foxman, U. Meirav, M.A. Kastner, Yigal Meir, Ned S. Wingreen, and S.J. Wind, Phys. Rev. Lett. **66**, 1926 (1996); E.B. Foxman, U. Meirav, P.L. McEuen, M.A. Kastner, O. Klein, P.A. Belk, D.M. Abusch, and S.J. Wind, Phys. Rev. B **50**, 14 193 (1994).

[10] M.A. Reed, J.N. Randall, R.J. Aggarwal, R.J. Matyi, T.M. Moore, and A.E. Wetsel, Phys. Rev. Lett. **60**, 535 (1998); C.G. Smith, M. Pepper, H. Ahmed, J.E.F. Frost, and D.G. Hasko, J. Phys. C **21**, L893 (1988).

[11] R.C. Ashoori, H.L. Stormer, J.S. Weiner, L.N. Pfeiffer, S.J. Pearton, K.W. Baldwin, and K.W. West, Phys. Rev. Lett. **68**, 3088 (1992).

[12] C.A. Stafford and Ned S. Wingreen, Phys. Rev. Lett. **76**, 1916 (1996).

[13] T. Pohjola, J. König, M.M. Salomaa, J. Schmid, H. Shoeller, and Gerd Schön, Europhys. Lett. **40**, 189 (1997).

[14] T. Ivanov, Europhys. Lett. **40**, 183 (1997).

[15] Kiyoshi Kawamura and Tomosuke Aono, Jpn. J. Appl. Phys., Part 1 **36**, 3951 (1997).

[16] Natan Andrei, Gergely T. Zimányi, and Gerd Schön, Phys. Rev. B **60**, R5125 (1999).

[17] M.R. Wegewijs and Yu.V. Nazarov, Phys. Rev. B **60**, 14 318 (1999).

[18] T. Aono, M. Eto, and K. Kawamura, J. Phys. Soc. Jpn. **67**, 1860 (1998); A. Georges and Yigal Meir, Phys. Rev. Lett. **82**, 3508 (1999).

[19] Ulrich Hohenester, Filippo Troiani, Elisa Molinari, Giovanna Panzarini, and Chiara Macchiavello, Appl. Phys. Lett. **77**, 1864 (2000).

[20] T.C. Au Yeung, W.Z. Shangguan, and Y.B. Yu (unpublished).

[21] Hao Chen, Jian Wu, Zhi-Qiang Li, and Yoshiyuki Kawazoe, Phys. Rev. B **55**, 1578 (1997).

[22] R. Ugajin, Phys. Rev. B **53**, 10 141 (1996).
[23] H. Sakaki, Jpn. J. Appl. Phys., Part 1 **28**, L314 (1989).
[24] K. Ismail, W. Chu, A. Yen, D.A. Antoniadis, and H.I. Smith, Appl. Phys. Lett. **54**, 460 (1989).
[25] A.-P. Jauho, Ned S. Wingreen, and Y. Meir, Phys. Rev. B **50**, 5528 (1994).
[26] To be precise, in the infinite dot case one cannot write $\vec{\Sigma}^r_{LL}$ as the form of G^{r0}_{11} defined in Eq. (17). But for notational and derivation convenience, one may still write formally $\vec{\Sigma}^r_{LL}$ in the form of G^{r0}_{11} as Eq. (17).
[27] E.N. Economou, *Green's Functions in Quantum Physics* (Springer-Verlag, Berlin, 1979), pp. 74–82.